

Article

# Fabrication and Characteristics of Heavily Fe-Doped LiNbO<sub>3</sub>/Si Heterojunction

Wencan Li <sup>1</sup>, Jiao Cui <sup>1</sup>, Dahuai Zheng <sup>1,\*</sup> , Weiwei Wang <sup>2</sup>, Shuolin Wang <sup>2</sup>, Shaoqing Song <sup>2</sup>, Hongde Liu <sup>2</sup> , Yongfa Kong <sup>1,2,\*</sup> and Jingjun Xu <sup>1,2</sup>

<sup>1</sup> The MOE Key Laboratory of Weak-Light Nonlinear Photonics and TEDA Institute of Applied Physics, Nankai University, Tianjin 300457, China

<sup>2</sup> School of Physics, Nankai University, Tianjin 300071, China

\* Correspondence: dhzheng@nankai.edu.cn (D.Z.); kongyf@nankai.edu.cn (Y.K.)

Received: 11 July 2019; Accepted: 19 August 2019; Published: 21 August 2019



**Abstract:** A series of heavily Fe-doped LiNbO<sub>3</sub> (LN:Fe) crystals were grown via the Czochralski method. The dark- and photo-conductivity of the 5.0 wt.% Fe-doped LiNbO<sub>3</sub> crystal reached  $3.30 \times 10^{-8} \Omega^{-1} \text{cm}^{-1}$  and  $1.46 \times 10^{-7} \Omega^{-1} \text{cm}^{-1}$  at 473 nm, which are about 7 and 5 orders of magnitude higher than that of congruent LiNbO<sub>3</sub>, respectively. Then, a p-n heterojunction was fabricated by depositing the heavily Fe-doped LiNbO<sub>3</sub> on a p-type Si substrate using the pulsed laser deposition. The current–voltage curve of the LN:Fe/Si heterojunction presents a well-defined behavior with a turn-on voltage of 2.9 V. This LN:Fe/Si heterojunction gives an excellent prototype device for integrated optics and electro-photonics.

**Keywords:** heavily Fe-doped; conductivity; pulsed laser deposition; heterojunction

## 1. Introduction

The concept of integrated optics has attracted wide interest all over the world, since Yariv suggested integrating photonic devices and electronic devices on the same substrate [1,2] in 1971. Integrating photonic and electronic active and passive components on silicon, now the commonly used substrate in integrated electronics, would make information or energy conversion, transmission, and reception much more efficient. A promising candidate material for such integration with Si substrate is lithium niobate (LiNbO<sub>3</sub>, LN), a well-known nonlinear optical crystal.

LN has many important properties such as electro-optic, acoustic-optic, thermoelectric, piezoelectric, and photorefractive effects. As a strong contender for "optical silicon", LN is applied for optical waveguides, electro-optical modulation, holographic storage, optical parametric oscillators, etc. [3–8]. However, LN is generally considered to be an insulator, and acts as a passive component in the above applications [9]. If LN devices can be integrated on silicon substrate to form an active component, then many excellent properties of LN can be applied to semiconductor integrated devices, which will embrace the benefits of both LN and semiconductor materials. The basic unit for an active component is a p-n junction. The low conductivity and absorption of LN were the main challenges posed to manufacturing an active component based on the p-n junction. In order to fabricate a device using LN, it is essential to develop a process that improves the conductivity of LN. The conductivity of LN can be greatly enhanced by introducing Fe into the crystal. However, when the concentration of Fe was below 0.1 wt.%, the conductivity was still very low when compared with semiconductors [10]. Then, it limited the future prospects for ferroelectric integrated devices.

In this work, the photo- and dark-conductivity in LN:Fe were increased several orders of magnitude further than that of the congruent LN (CLN) by heavily doping Fe [11,12]. A heterojunction of LN:Fe

deposited on the p-type Si substrate was fabricated with good rectifying properties. This heterojunction provides a promising prospect for the multi-functional applications of passive and active integration.

## 2. Experimental Details

### 2.1. Samples Preparation

A series of LN crystals doped with 1.0, 3.0 and 5.0 wt% Fe<sub>2</sub>O<sub>3</sub> (labeled as LN:Fe<sub>1</sub>, LN:Fe<sub>3</sub> and LN:Fe<sub>5</sub>, respectively) were grown using the Czochralski method. These grown crystals were polarized, cut to 5.0 × 6.0 × 4.5 mm<sup>3</sup> (X × Y × Z) pieces, and optically polished. In addition, the dopant concentrations given were nominal values, and we cut all the samples from the top of the crystal boule. This ensured as much consistency as possible between the actual and nominal composition of the crystal. In the conductivity measurement, a series circuit was applied on the XY-planes, pasting silver glue as electrodes. The samples were placed in an electrostatic shield to get the dark-conductivity. LN:Fe thin film was deposited on a p-type Si (100) wafer by the pulsed laser deposition (PLD) to obtain a p-n junction. Before deposition, the single side polished Si substrate was ultrasonically cleaned for 10 min in alcohol, acetone, and deionized water, respectively. Then the target of *c*-cut LN:Fe<sub>5</sub> single crystal and the Si substrate were placed together in a vacuum chamber with a distance of 6.0 cm between them. The chamber was pumped to 10<sup>-5</sup> Pa and the substrate was heated to 700 °C to keep for 10 min in order to remove the impurities on the surface. The deposition processing lasted 2 h, while the substrate's temperature of 600 °C and the ambient gas of 30 Pa oxygen were kept. KrF excimer laser operating at 248 nm and 25 ns duration time was used as a light source. The laser with energy density of 1.5 J/cm<sup>2</sup> was focused at an angle of 45° on the surface of the rotating crystal target. The pulse frequency of the laser was 3 Hz. After deposition, annealing in situ was presented in 10<sup>5</sup> Pa oxygen pressure for 30 min.

### 2.2. Measurements

The absorption of the LN:Fe crystals was measured by a U-4100 Spectrophotometer (Hitachi Science and Technology, Tokyo, Japan). X-ray diffraction (XRD) patterns were measured using a Bruker D8 Advances X-ray Diffractometer (Karlsruhe, Germany). The current-voltage (I-U) curves were measured by a Source Meter (KEITHLEY 6517A, Cleveland, OH, USA). To measure the photoconductivity, a laser with a wavelength of 473 nm and intensity of 1.8 W/cm<sup>2</sup> passed through the polished XZ-block in a dark room.

## 3. Results and Discussion

### 3.1. Absorption Spectrum and Conductivity of LN:Fe Crystals

The absorption spectra of LN:Fe crystals were measured by a U-4100 Spectrophotometer at room temperature (25 °C). During the measurement, the light is incident vertically onto a sample (0.5 mm optical polished y-cut plate), and we get the transmittance spectrum. Based on the Mclean equation [13], the absorption coefficient ( $\alpha$ ), transmittance (T), and reflectance (R) satisfy the following relationships:

$$\alpha(\lambda) = \frac{-1}{d} \ln \left( -b + \sqrt{b^2 + \frac{1}{R^2}} \right) \quad (1)$$

$$R = \frac{(n-1)^2}{(n+1)^2} \quad (2)$$

$$b = \frac{(1-R)^2}{2TR^2} \quad (3)$$

$n$  is the refractive index of incident light in the crystal, which can be calculated according to the Semeller equation [14]. We can then get the absorption coefficient from the transmittance spectrum.

As shown in Figure 1a, there is an absorption peak at 477 nm in the spectrum of LN:Fe<sub>1</sub>, while there is an even stronger absorption around the 477 nm in the LN:Fe<sub>3</sub> and LN:Fe<sub>5</sub>. Compared with LN:Fe<sub>1</sub>, the wide infrared peak of LN:Fe<sub>3</sub> and LN:Fe<sub>5</sub> at around 1100 nm is much stronger, which corresponds to the absorption band of free polarons Nb<sup>4+</sup><sub>Li</sub> [15,16]. Meanwhile, Figure 1a shows that the absorption edges of LN:Fe are redshift with increased doping concentration (from 1.0 wt.% to 5.0 wt.%). In fact, visible and ultraviolet light are almost absorbed in the spectra of LN:Fe<sub>3</sub> and LN:Fe<sub>5</sub>, and the absorption of infrared light enhances remarkably in LN:Fe<sub>5</sub>.

The results indicate that the absorption region of LN has been enhanced from ultraviolet to infrared band by Fe doping, which makes the excitation of the p-n junction become more selective. In other respects, the heavily Fe-doped LN may be a promising solar energy material, used to improve photoelectric absorption and conversion efficiency due to its excellent optical absorption properties.

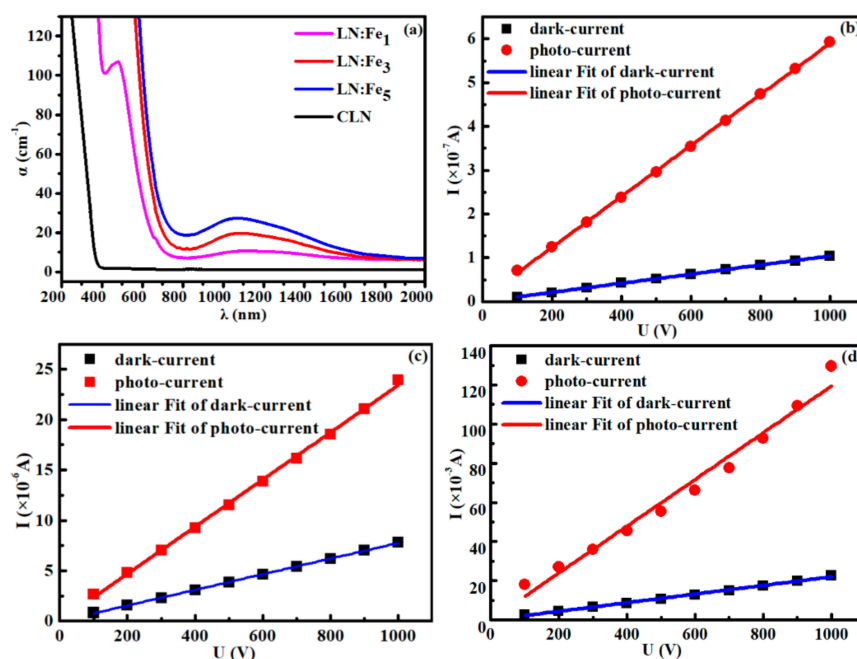


**Figure 1.** (a) The absorption spectra of y-cut LN:Fe and CLN, (b–d). The current versus voltage (I-U) curves of (b) LN:Fe<sub>1</sub>, (c) LN:Fe<sub>3</sub>, and (d) LN:Fe<sub>5</sub> blocks, the dark-current in a dark room, and the photo-current with the optical intensity at  $\lambda = 473$  nm were measured, respectively.

The current versus voltage (I-U) curves of LN:Fe are shown in Figure 1b–d. We can see that the photo-current of the LN:Fe is much larger than its dark-current at the same voltage. The dark-conductivity ( $\sigma_d$ ) and photo-conductivity ( $\sigma_{ph}$ ) are shown in Table 1. As shown in Figure 1d, especially for LN:Fe<sub>5</sub>, the dark- and photo- conductivity reach  $3.30 \times 10^{-8} \Omega^{-1} \text{cm}^{-1}$  and  $1.46 \times 10^{-7} \Omega^{-1} \text{cm}^{-1}$  respectively, which are about 7 and 5 orders of magnitude higher than that of CLN ( $5.0 \times 10^{-15} \Omega^{-1} \text{cm}^{-1}$  for dark-conductivity [11] and  $10^{-12} \Omega^{-1} \text{cm}^{-1}$  for photo-conductivity [12]).

Based on the above results, the LN:Fe<sub>5</sub> crystal shows the nice absorption and enhanced conductivity properties, which may be contributed to the concentration of Fe<sup>3+</sup> and Fe<sup>2+</sup> and their ratio in LN. However, as the Fe doping concentration increases, it becomes difficult to grow high quality doped LN crystals. It is worth increasing the Fe doping concentration, which we can try to realize through improving the crystal growth process or preparing the target using the solid-state sintering of powder method. In addition, the results attract us to construct a heterojunction with the n-type LN layer and the p-type Si layer, which provides the possibility of integrated optical devices based on LN.

**Table 1.** The dark- and photo-conductivity of LN doped with 1.0, 3.0, and 5.0 wt.% Fe<sub>2</sub>O<sub>3</sub>. A 473 nm laser with light intensity of 1.8 W/cm<sup>2</sup> was applied to the measurement of photo-conductivity.

Crystal	$\sigma_d$ ( $\Omega^{-1} \text{ cm}^{-1}$ )	$\sigma_{ph}$ ( $\Omega^{-1} \text{ cm}^{-1}$ )
LN:Fe <sub>1</sub>	$1.56 \times 10^{-10}$	$7.70 \times 10^{-10}$
LN:Fe <sub>3</sub>	$1.16 \times 10^{-8}$	$2.35 \times 10^{-8}$
LN:Fe <sub>5</sub>	$3.30 \times 10^{-8}$	$1.46 \times 10^{-7}$
CLN	$5.0 \times 10^{-15}$ [11]	$10^{-12}$ [12]

### 3.2. LN:Fe<sub>5</sub>/Si p-n Junction and Its Rectification Characteristics

A p-n junction of LN:Fe<sub>5</sub>/Si was manufactured by PLD. The film thickness controlled by deposition time is about 2.0  $\mu\text{m}$ , which can be measured by a step profiler. The XRD patterns of the substrate (above) and the p-n junction (below) are shown in Figure 2. Si(100) peak of the substrate is found at 69.1°. Except for the peak of the substrate, a stronger peak of LN:Fe<sub>5</sub>(006) at 39.1° was simultaneously measured. The full width half maximum (FWHM) of the (006) orientation of LN:Fe<sub>5</sub> is about 0.37°, which is less than the FWHM value (1.4°) of the undoped films of LN single crystal [17]. The results indicate c-axis oriented LN film with very few flaws was successfully deposited on the Si substrate.

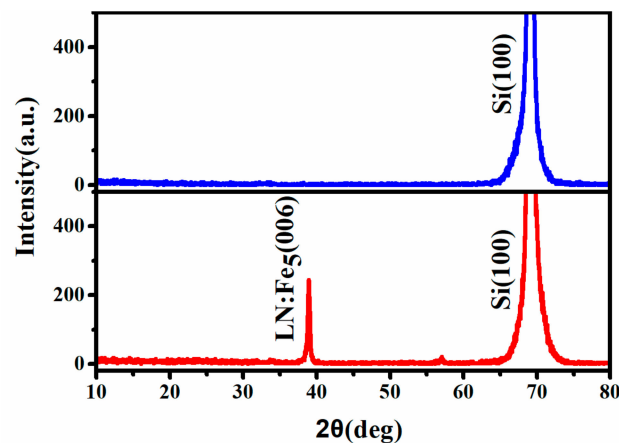


**Figure 2.** X-ray diffraction (XRD) patterns for LN:Fe<sub>5</sub>/Si p-n junction, the diffraction peak (above) at  $2\theta = 69.1^\circ$  corresponds to the Si(100) substrate and the peaks labeled LN:Fe<sub>5</sub>(006) and Si(100) (below) correspond to LN:Fe<sub>5</sub> thin film at  $2\theta = 39.1^\circ$  and Si substrate  $2\theta = 69.1^\circ$ .

Figure 3a is the schematic diagram of the experimental setup of LN:Fe<sub>5</sub>/Si p-n junction for measuring current-voltage (I-U), and its rectifying property is shown in Figure 3b. As the film is very thin, the relaxation time of the p-n junction is less than 10 seconds and the LN:Fe<sub>5</sub>/Si p-n junction is stable. Obviously, good rectifying property with a turn-on voltage of 2.9 V for the forward voltage was measured. A breakdown voltage of  $-6$  V was also shown in Figure 3b.

Based on the above results, we can find that the LN:Fe<sub>5</sub>/Si presents obvious rectifying characteristics with a turn-on voltage of 2.9 V and a breakdown voltage of  $-6$  V. For a typical SOI-type p-n junction, which exhibits a turn-on voltage of 2.2 V and a breakdown voltage of 550–770 V [18], many factors need to be considered in evaluating its performance. In any case, for the LN:Fe<sub>5</sub>/Si, the turn-on voltage and the breakdown voltage are less desirable. Further research is ongoing to optimize the heterojunction performance.

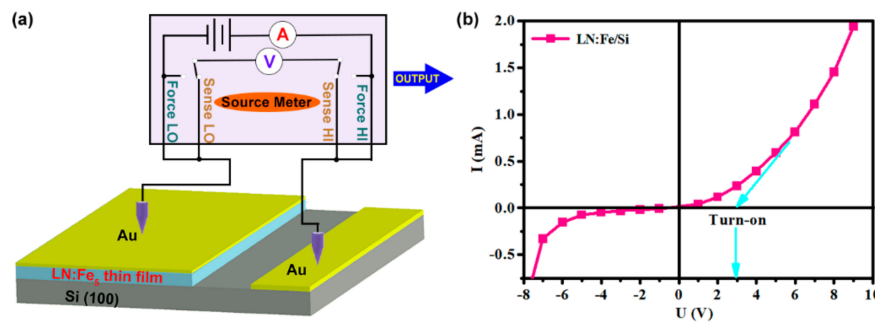


**Figure 3.** (a) Schematic diagram of the experimental setup for p-n junction LN:Fe<sub>5</sub>/Si. (b) The current-voltage curve of the LN:Fe<sub>5</sub>/Si junction with a turn-on voltage of 2.9 V for the forward voltage and a breakdown voltage of about −6 V.

### 3.3. Energy Band Diagram of the LN:Fe<sub>5</sub>/Si p-n Junction

To understand the rectifying property, the energy band diagram of the p-n junction was studied. Figure 4a shows the energy band diagram of isolated p-type Si and n-type LN:Fe<sub>5</sub>. The work function of heavily doped p-type Si was reported as  $W_{Si} = 5.00$  eV [19] and the band gap of Si is approximately 1.11 eV [20]. CLN film deposited by PLD is usually Li-deficient and the band gap and electron affinity ( $\chi$ ) of LN were still regarded as 3.90 eV and 1.10 eV [21–23]. That is to say, the impurity defects in LN do not change its intrinsic band gaps and electron affinity energy significantly, but they introduce defect level. So we consider that the band gaps and electron affinity energy of LN:Fe<sub>5</sub> are approximately 3.90 eV and 1.10 eV, and the gap ( $E_n$ ) between conduction band ( $E_C$ ) and fermi level ( $E_F$ ) of the LN:Fe<sub>5</sub> is as follows:

$$(E_n)_{LN:Fe5} = E_C - E_F = 1.30 \text{ eV} \quad (4)$$

The work function of LN:Fe<sub>5</sub> is approximately calculated according to Equation (5):

$$W_{LN:Fe5} = \chi + (E_n)_{LN:Fe5} = 2.40 \text{ eV} \quad (5)$$

As shown in Figure 4b, when two kinds of materials are combined, the energy band bending occurs. The value of the bending energy is determined on the work function according to Equation (6):

$$\Delta E = W_{Si} - W_{LN:Fe5} = 2.60 \text{ eV} \quad (6)$$

Since the carriers in Si are much more than that in LN, band bending falls mainly in LN and forms the potential barrier, which is close to the value of turn-on voltage 2.9 V. In other words, an energy of 2.60 eV is necessary to get a forward current.

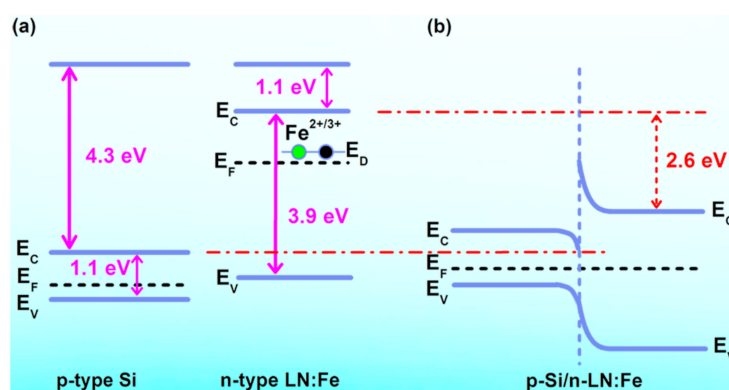


**Figure 4.** (a) Energy band diagram of isolated p-type Si and n-type LN:Fe<sub>5</sub>. (b) Energy band diagram of ideal LN:Fe<sub>5</sub>/Si heterojunction at thermal equilibrium.

#### 4. Conclusions

In summary, up to 5.0 wt.% Fe<sub>2</sub>O<sub>3</sub> doped LiNbO<sub>3</sub> crystals were grown. The conductivity of LN:Fe was greatly increased by 7 (dark-conductivity) and 5 (photo-conductivity) orders of magnitude compared with CLN. A p-n junction of LN:Fe<sub>5</sub>/Si was fabricated via the PLD method. The LN:Fe<sub>5</sub>/Si presents the rectifying characteristic with a turn-on voltage of 2.9 V for the forward voltage and a breakdown voltage of −6 V for the backward voltage. The energy band diagram indicates that an energy of 2.60 eV is necessary to get a forward current. The LN:Fe<sub>5</sub>/Si heterojunction gives an excellent prototype device for integrated optics and electro-photonics.

**Author Contributions:** Conceptualization, D.Z., Y.K., and J.X.; Funding acquisition, D.Z. and Y.K.; Investigation, W.L., J.C., S.W., and S.S.; Methodology, J.C.; Writing—original draft, W.L. and J.C.; Writing—review and editing, W.L., D.Z., W.W., S.W., S.S., H.L. and Y.K.

**Funding:** This research was funded by the National Natural Science Foundation of China with grant number [11674179] and [61705116] and the Program for Changjiang Scholars and Innovative Research Team in University with grant number [IRT\_13R29].

**Conflicts of Interest:** The authors declare no conflict of interest.

#### References

1. Chen, H.; He, Z.; Wang, W. Design of a multi-mode interference crossing structure for three periodic dielectric waveguides. *Prog. Electromagn. Res. Lett.* **2018**, *75*, 47–52. [[CrossRef](#)]
2. Yariv, A. *Introduction to Optical Electronics*; Holt, Rinehart and Winston: Boston, MA, USA, 1971.
3. Berciano, M.; Marcaud, G.; Damas, P.; Roux, X.L.; Crozat, P.; Ramos, C.A.; Galacho, D.P.; Benedikovic, D.; Marris-Morini, D.; Cassan, E.; et al. Fast linear electro-optic effect in a centrosymmetric semiconductor. *Commun. Phys.* **2018**, *1*, 2399–3650. [[CrossRef](#)]
4. Bonfadini, S.; Ciciulla, F.; Criante, L.; Zaltron, A.; Simoni, F.; Reshetnyak, V.; Lucchetti, L. Optofluidic platform using liquid crystals in lithium niobate microchannel. *Sci. Rep.* **2019**, *9*, 1062. [[CrossRef](#)]
5. Cai, L.; Gorbach, A.V.; Wang, Y.; Hu, H.; Ding, W. Highly efficient broadband second harmonic generation mediated by mode hybridization and nonlinearity patterning in compact fiber-integrated lithium niobate nano-waveguides. *Sci. Rep.* **2018**, *8*, 12478. [[CrossRef](#)]
6. Li, W.; Ji, L.J. Perovskite ferroelectrics go metal free. *Science* **2018**, *361*, 132. [[CrossRef](#)] [[PubMed](#)]
7. Von Hoegen, A.; Mankowsky, R.; Fechner, M.; Forst, M.; Cavalleri, A. Probing the interatomic potential of solids with strong-field nonlinear phononics. *Nature* **2018**, *555*, 79–82. [[CrossRef](#)]
8. Jin, Y.; Zhang, N.; Zhang, B. Fabrication of p-type ZnO:N films by oxidizing Zn<sub>3</sub>N<sub>2</sub> films in oxygen plasma at low temperature. *Materials* **2017**, *10*, 236. [[CrossRef](#)] [[PubMed](#)]
9. Kong, Y.; Bo, F.; Wang, W.; Zheng, D.; Liu, H.; Zhang, G.; Rupp, R.; Xu, J. Recent progress in lithium niobate: Optical damage, defect simulation, and on-chip devices. *Adv. Mater.* **2019**, 1806452. [[CrossRef](#)]
10. Falk, M.; Japs, J.; Woike, T.; Buse, K. Charge transport in highly iron-doped oxidized lithium niobate single crystals. *Appl. Phys. B* **2007**, *87*, 119–122. [[CrossRef](#)]
11. Luedtke, F.; Villarroel, J.; García-Cabañes, A.; Buse, K.; Carrascosa, M. Correlation between photorefractive index changes and optical damage thresholds in z-cut proton-exchanged-LiNbO<sub>3</sub> waveguides. *Opt. Express* **2009**, *17*, 658–665. [[CrossRef](#)]
12. Göring, R.; Zhan, Y.; Steinberg, S. Photoconductivity and photovoltaic behavior of LiNbO<sub>3</sub> and LiNbO<sub>3</sub> waveguides at high optical intensities. *Appl. Phys. A* **1992**, *55*, 97–100. [[CrossRef](#)]
13. Kovács, L.; Ruschhaupt, G.; Polgár, K.; Corradi, G.; Wöhlecke, M. Composition dependence of the ultraviolet absorption edge in lithium niobate. *Appl. Phys. Lett.* **1997**, *70*, 2801. [[CrossRef](#)]
14. Schlarb, U.; Betzler, K. Refractive indices of lithium niobate as a function of temperature, wavelength, and composition: A generalized fit. *Phys. Rev. B* **1993**, *48*, 15613–15620. [[CrossRef](#)] [[PubMed](#)]
15. Merschjann, C.; Berben, D.; Imlau, M.; Wöhlecke, M. Evidence for two-path recombination of photoinduced small polarons in reduced LiNbO<sub>3</sub>. *Phys. Rev. Lett.* **2006**, *96*, 186404. [[CrossRef](#)] [[PubMed](#)]
16. Sasamoto, S.; Hirohashi, J.; Ashihara, S. Polaron dynamics in lithium niobate upon femtosecond pulse irradiation: Influence of magnesium doping and stoichiometry control. *J. Appl. Phys.* **2009**, *105*, 083102. [[CrossRef](#)]

17. Gonzalo, J.; Chaos, J.A.; Suárez-García, A.; Afonso, C.N.; Pruneri, V. Enhanced second-order nonlinear optical response of LiNbO<sub>3</sub> films upon Er doping. *Appl. Phys. Lett.* **2002**, *81*, 2532–2534. [[CrossRef](#)]
18. Kinoshita, T.; Nagashima, T.; Obata, T.; Takashima, S.; Yamamoto, R.; Togashi, R.; Kumagai, Y.; Schlessler, R.; Collazo, R.; Koukitu, A.; et al. Fabrication of vertical Schottky barrier diodes on n-type freestanding AlN substrates grown by hydride vapor phase epitaxy. *Appl. Phys. Express* **2015**, *8*, 061003. [[CrossRef](#)]
19. Novikov, A. Experimental measurement of work function in doped silicon surfaces. *Solid State Electron* **2010**, *54*, 8–13. [[CrossRef](#)]
20. Streetman, B.G.; Banerjee, S. *Solid State Electronic Devices*; Prentice Hall: Englewood Cliffs, NJ, USA, 1995.
21. Yang, W.C.; Rodriguez, B.J.; Gruverman, A.; Nemanich, R.J. Polarization-dependent electron affinity of LiNbO<sub>3</sub> surfaces. *Appl. Phys. Lett.* **2004**, *85*, 2316–2318. [[CrossRef](#)]
22. Hao, L.; Li, Y.; Zhu, J.; Wu, Z.; Deng, J.; Liu, X.; Zhang, W. Fabrication and electrical properties of LiNbO<sub>3</sub>/ZnO/n-Si heterojunction. *AIP Adv.* **2013**, *3*, 042106. [[CrossRef](#)]
23. Guo, S.M.; Zhao, Y.G.; Xiong, C.M.; Lang, P.L. Rectifying IV characteristic of LiNbO<sub>3</sub>/Nb-doped SrTiO<sub>3</sub> heterojunction. *Appl. Phys. Lett.* **2006**, *89*, 223506. [[CrossRef](#)]



© 2019 by the authors. Licensee MDPI, Basel, Switzerland. This article is an open access article distributed under the terms and conditions of the Creative Commons Attribution (CC BY) license (<http://creativecommons.org/licenses/by/4.0/>).